Original papers

Med Ultrason 2026, Vol. 28, no. 3, 293-300
DOI: 10.11152/mu-4589

Diagnostic value of ultrasound parameters combined with clinical features in children with alveolar and non-alveolar rhabdomyosarcoma

Nana Li, Ting Wang, Tianzi Li, Bailing Liu

Department of Ultrasound, Xi'an Children's Hospital, Xi'an, China

Abstract

Aims: The aim of this study was to investigate the differences in clinical and ultrasound findings between alveolar rhabdomyosarcoma (ARMS) and non-ARMS in order to improve the accuracy of preoperative diagnosis of ARMS in children. **Material and methods:** A retrospective study of 33 children with pathologically confirmed RMS (ARMS and non-ARMS groups) was realized. Clinical features and ultrasound parameters were compared between ARMS and non-ARMS using Fisher 's exact test analysis. Receiver operating characteristic (ROC) curves and area under the curve (AUC) were used to represent diagnostic performance. **Results:** Among the clinical features, there were statistically significant differences between ARMS and non-ARMS groups in site (p=0.020), TNM stage (p=0.007), IRS stage (p=0.009), risk grade (p=0.011), and distant metastasis (p=0.020). There were statistical differences in necrosis (p= p0.039) and central hyperechoic fiber bundles (p<0.001) between the two groups. The combination of ultrasound and clinical characteristics demonstrated excellent predictive ability (AUC was 0.964). **Conclusions:** Children with ARMS more often present with poor prognosis, and combined clinical and ultrasound features are helpful for preoperative identification of ARMS and providing imaging evidence for accurate clinical diagnosis and treatment.

Keywords: rhabdomyosarcoma; alveolar rhabdomyosarcoma; ultrasound; children

Introduction

Rhabdomyosarcoma (RMS) is a rare malignant soft tissue tumor originating from striated muscle cells or immature mesenchymal cells that are about to differentiate into striated muscle. It is the most common soft tissue sarcoma in children [1]. Its incidence is second only to neuroblastoma and Wilms' tumor, accounting for approximately 3% of all malignant tumors and 6.5% of soft tissue sarcomas in children in China [2]. RMS is seen at any age in children, and its high incidence is in the age range of 1-4 years, and the incidence is higher in males than in females [3]. Because RMS originates from interstitial cells in the embryonic period, it can occur anywhere in the body, most commonly in the head and neck region and genitourinary tract, followed by involvement of the extremities, trunk, retroperitoneum, and biliary tract [4]. The clinical symptoms of RMS are related to the site of tumor growth, and most of the children present with rapidly growing soft tissue masses.

According to the pathological results, WHO divides RMS into four subtypes: embryonal rhabdomyosarcoma (ERMS), alveolar rhabdomyosarcoma (ARMS), pleomorphic rhabdomyosarcoma (PRMS), and spindle cells/sclerosing rhabdomyosarcoma (SRMS/ScRMS) [5]. ERMS and ARMS are the most common in children, accounting for about 70-80%. RMS histomorphology is diverse, and its prognosis is associated with the age,

Received 29.10.2025 Accepted 18.01.2026
Early Access publication date 10.02.2026
Med Ultrason
2026, Vol. 28, No 3, 293-300
Corresponding author: Bailing Liu, MD
Department of Ultrasound,
Xi'an Children's Hospital,
69 Xijuyuan Road,
Lianhu District, Xi'an, 710003,
China
Email: bailingliu168@163.com

tumor size, clinical stage, pathological type, distant metastasis, and specific genetic changes of the child [6-8]. Primary RMS in bladder, prostate, limbs, trunk and other parts has a poor prognosis. ARMS is a small round cell tumor with high malignancy and invasiveness, which is prone to hematogenous metastasis of regional lymph node metastasis due to poor tumor cell differentiation, suggesting a poor prognosis [9]. Previous studies have shown that PAX3/7-FOXO1 gene fusion exists in about 80% of ARMS, which promotes tumor proliferation and metastasis by activating downstream signaling pathways, and the five-year survival rate of children with positive fusion genes is significantly lower than that of negative fusion genes [10,11]. At the same time, mutations and abnormal miRNA expression in ARMS are associated with prognosis [12]. Comprehensive treatment is currently the standard approach for RMS patients. In addition to patients who are eligible for complete curative surgical resection, maintenance chemotherapy for high-risk RMS has been shown to improve survival outcomes [13].

RMS lacks distinct imaging features and laboratory tests, and is difficult to differentiate from other solid tumors due to the heterogeneity or differentiation of the tumor, especially large abdominal and pelvic tumors in young infants. The gold standard for defining the nature of the tumor is histopathological examination, but this invasive examination is usually accompanied by other complications. Therefore, for children with RMS, especially ARMS, preoperative determination of the nature of the tumor is essential for the treatment and prognosis of children. Conventional ultrasound (US) of RMS usually presents as a solid mass with infiltrative growth, which can involve grade adjacent tissue, and internal echoes also show diversity due to heterogeneous cellular distribution within the tumor. RMS is commonly located in or around the muscle layer. Sheng et al found that calcification, encapsulated vessels, and intraspinal tumor extension were less common in RMS children compared with neuroblastoma [14]. Franco et al analyzed computed tomography (CT) and magnetic resonance imaging (MRI) images of 14 children with RMS and found that their imaging features (such as density and heterogeneity) were not associated with its pathological subtypes [15]. According to previous studies, there have been no studies to definitively focus the diagnostic efficacy of US in RMS in children, especially ARMS with poor prognosis. The aim of this study was to investigate the differences in clinical and US features between ARMS and non-ARMS in order to improve the accuracy of preoperative diagnosis of ARMS in children and to provide imaging evidence for clinical treatment and intervention.

Material and methods

Study population

A retrospective analysis was conducted on 33 children with pathologically confirmed RMS from January 2019 to March 2025 at Xi'an Children's Hospital. The institutional Ethics Committee approved the study of our hospital. Since this study was retrospective, all patients waived informed consent. The inclusion criteria were as follows: a) patients diagnosed as RMS by pathological examination after surgery or biopsy; b) patients who underwent US examination 2 weeks before surgery. The exclusion criteria were as follows: a) patients with incomplete clinical data; b) patients who had missing preoperative US images and poor image quality; c) patients with history of other malignant tumors at admission; d) patients who did not undergo histopathological examination.

US acquisition and analysis

US image was performed using a Philips EPIQ 7 Color Doppler Ultrasound System with high frequency probe (linear array probe L12-5) and low frequency probe (convex array probe C5-1). First, low-frequency probe was used to determine the target lesion, evaluate its size, boundary and shape, high-frequency probe was used to observe the echo inside the lesion and its relationship with the surrounding tissues; color Doppler flow imaging (CDFI) was used to assess the blood flow of the lesion.

US examinations were performed by a single sonographer with 3 years of experience in ultrasound. The final analysis of ultrasound images was performed by two sonographers with more than 5 years of ultrasound experience in pediatric diseases. In order to maintain the objectivity of the image results, they were blinded to the pathological results of the children. We assessed the US characteristics of each RMS patient and extracted lesion characteristics from US images, including: site, maximum lesion diameter, echogenicity (iso-/hypo-/mixed-), shape (irregular/lobulated/regular), margin (clear/unclear), calcification (presence/absence), necrosis (presence/absence), central hyperechoic fiber bundles (presence/absence), invasion of theadjacent tissues (presence/absence), and Adler flow grade (grade 0/I/II/III).

Diagnosis and pathological assessment

According to the international and domestic guidelines for the diagnosis and treatment of RMS in children and adolescents [2], we first performed clinical evaluation in children with suspected RMS, then localization and qualitative diagnosis by imaging examination (including US/CT/MRI), and finally confirmed the diagnosis and pathological classification by US-guided biopsy

or surgical pathology. In this study, we first selected RMS children who underwent US while they underwent CT or MRI (head/chest/abdomen) to determine if metastases occurred elsewhere. During the whole process, the clinical data of the children were obtained by reviewing the case system, while US images were obtained from the Picture Archiving and Communication System (PACS). We used the tumor node metastasis classification (TNM) staging system and the Intergroup Rhabdomyosarcoma Study Group (IRS) staging system to stage RMS [16,17]. TNM staging system is based on the primary location, size, lymph node metastasis or distant metastasis of the tumor and other conditions for staging. The IRS staging system is staged according to the extent of surgical resection and postoperative pathological microscopic results: stage I refers to the tumor showing localized lesions, which can be completely removed by surgery without regional lymph node metastasis; stage II refers to the flesh eye showing complete resection of the tumor, but also that there has been local tissue invasion or regional lymph node metastasis around, with or without microscopic residual; stage III refers to the tumor that cannot be completely removed or only biopsy is performed, residual tumor tissue can be seen macroscopically, with microscopic residual; and stage IV refers to distant metastasis already at the time of diagnosis. Combined with IRS clinical staging criteria and histopathological classification, RMS was divided into three groups: low, intermediate, and high risk.

Treatment

The pathological nature of the tumor is determined through surgical resection or US-guided needle biopsy. Surgical resection is the preferred treatment for complete removal of the tumor. In cases where resection is difficult or where function needs to be preserved, adjuvant chemotherapy may be administered after confirmation by biopsy.

Statistical analyses

All analyses were performed using SPSS 26.0 statistical software (IBM Corp., Armonk, NY, USA). The Kolmogorov Smirnov test was used to assess the normality of continuous variables. Student's test and Mann-Whitney U test were employed for normally distributed and non-normally distributed continuous variables, respectively. Results were reported as mean±standard deviation for normally distributed variables and as median with interquartile range for non-normally distributed variables. Categorical variables were evaluated using the chi-square test. A two-tailed p-value of <0.05 was considered statistically significant. Receiver operating characteristic (ROC) curves and area under the curve (AUC) were used to represent diagnostic performance.

Results

Clinical characteristics analysis and pathological type

Based on pathological results, 33 children with RMS were ultimately classified as either ARMS or non-ARMS. Of the children in this group, 17 (51.5%, 17/33) were male, with age of onset of 1 month – 15 years, mean age of 5.3 ± 4.3 years, and a median age of 4.0 years (Table I). The pathological types and clinical stages of 33 patients in this group are shown in table II. Among the clinical features, there were statistically significant differences between ARMS and non-ARMS groups in site (p=0.020), TNM stage (p= 0.007), IRS stage (p= 0.009), risk grade (p=0.011), and distant metastasis (p=0.020).

Analysis of US characteristics of ARMS and non-ARMS

In US all 33 cases of RMS showed ill-defined borders and irregular shape. Due to large tumor diameter hypo- or mixed echogenicity was predominant. Grade II-III blood flow signals were more frequently found (84.8% vs 15.2%). Table III shows the comparison of US characteristics between ARMS and non-ARMS. Compared with the non-ARMS group, the ARMS group more often showed mixed echoes (75.0% vs. 19.0%), and there were statistically significant differences between the two groups in necrosis (p=0.039) and central hyperechoic fiber bundles (p<.001) (fig 1-3). There were no statistically significant differences in border, shape, blood flow grade, calcification, and invasion of surrounding tissues.

Evaluation of diagnostic performance

We used the ROC curve to evaluate diagnostic performance (fig 4), and the results showed that US features demonstrated good predictive ability. The AUC value for necrosis was 0.690 (95%CI: 0.497–0.884), with diagnostic sensitivity and specificity of 66.7% and 71.4%, respectively. The AUC value for central hyperechoic fiber bundles was 0.845 (95%CI: 0.694–0.997), with diagnostic sensitivity and specificity of 83.3% and 85.7%, respectively. We combined all US features and all clinical features separately and compared their predictive capabilities. The results showed that the diagnostic performance of combining all US and clinical features was superior to that of using a single feature (AUC values of 0.964, 0.845, and 0.865, respectively) (Table IV).

Treatment and Follow-up

In our study 7 children (7/33, 21.2%) underwent both surgical resection and chemotherapy, 22 children (22/33, 66.7%) were assessed as inoperable and received chemotherapy alone, and 4 children (4/33, 12.1%) discontinued treatment. Follow-up was conducted for 29 children who received treatment. Among them, 23 (23/29, 79.3%)

Table I. Comparison of clinical characteristics between ARMS and non-ARMS

Variables	ARMS (n=12)	Non-ARMS (n=21)	p value
Gender, male	8 (66.7%)	9 (42.9%)	0.170
Age	5.9±4.6	4.9±4.1	0.516
Site			0.020
Abdomen	6 (50.0%%)	13 (61.9%)	
Head and neck	2 (16.7%)	8 (38.1%)	
Other	4 (33.3%)	0 (0.0%)	
TNM stage			0.007
1	0 (0%)	2 (9.5%)	
2	1 (8.3%)	7 (33.3%)	
3	3 (25.0%)	7 (33.3%)	
4	8 (66.7%)	5 (23.8%)	
IRS stage			0.009
II	0 (0%)	4 (19.0%)	
III	4 (33.3%)	12 (57.1%)	
IV	8 (66.7%)	5 (23.8%)	
Risk class			0.011
Low Risk	0 (0%)	6 (28.6%)	
Intermediate risk	4 (33.3%)	9 (42.9%)	
High risk	8 (66.7%)	6 (28.6%)	
Metastasis, present	8 (66.7%)	5 (23.8%)	0.020

ARMS, alveolar rhabdomyosarcoma; TNM, tumor node metastasis classification; IRS, Intergroup Rhabdomyosarcoma Study Group

showed tumor shrinkage or no progression post-treatment, 6 (6/29, 20.7%) experienced progression or recurrence. Among children with progression or recurrence, pathologic classification was ARMS in 4 cases (4/6, 66.7%).

Discussion

The most common soft tissue tumor in childhood is RMS, and its site of growth and clinical presentation are diverse [18]. ARMS generally indicates a poor prognosis and poor patient survival [19]. In this paper, we compared the clinical and US characteristics of ARMS with non-ARMS, and the results showed that among the clinical characteristics, ARMS group and non-ARMS group were statistically different in site, TNM stage, IRS stage, risk grade and distant metastasis. There were statistically significant differences between the two groups in the necrosis and central hyperechoic fiber bundles. Combining all US and clinical features resulted in excellent predictive ability (AUC=0.964).

RMS can occur anywhere, mostly in skeletal muscles of the extremities in adults, while in children mostly in non-skeletal muscles, most commonly in the head and neck region, and genitourinary tract. Of the 33 RMS patients in this study, 8 were primary in the maxillofacial region and 16 were primary in the pelvic cavity, consistent with previous report [20]. The clinical symptoms of RMS vary according to the site of disease, and most abdominal or pelvic tumors present with abdominal distension or associated urogenital symptoms. Primary tumors

Table II. Pathological classification and IRS staging statistics

Pathological type	IRS stage			Total
	II	III	IV	
ERMS	3	9	5	17
ARMS	0	4	8	12
SRMS	1	3	0	4
Total	4	16	13	33

ERMS, embryonal rhabdomyosarcoma; ARMS, alveolar rhabdomyosarcoma; SRMS, sclerosing rhabdomyosarcoma

Table III. Comparison of ultrasound characteristics between ARMS and non-ARMS

Variables	ARMS (n=12)	Non-ARMS (n=21)	p value
Maximum lesion diameter	79.2±34.6	67.2±28.3	0.286
Echogenicity			0.880
hyper-	3 (25.0%)	15 (71.4%)	
mixed-	9 (75.0%)	4 (19.0%)	
iso-	0 (0%)	2 (9.5%)	
Margin			0.355
clear	3 (25.0%)	8 (38.1%)	
indistinct	9 (25.0%)	13 (61.9%)	
Shape			0.640
regular	1 (8.3%)	3 (14.3%)	
lobulated	1 (8.3%)	3 (14.3%)	
irregular	10 (83.3%)	15 (71.4%)	
Adler flow grade			0.612
0-I	2 (16.7%)	3 (14.3%)	
II-III	10 (83.3%)	18 (85.7%)	
Necrosis			0.039
absence	4 (33.3%)	15 (71.4%)	
presence	8 (66.7%)	6 (28.6%)	
Calcification			0.294
absence	10 (83.3%)	20 (95.2%)	
presence	2 (16.7%)	1 (4.8%)	
Central hyperechoic fiber bundles			<0.001
absence	2 (16.7%)	18 (85.7%)	
presence	10 (83.3%)	3 (14.3%)	
Invasion of adjacent tissues			0.124
absence	2 (16.7%)	9 (42.9%)	
presence	10 (83.3%)	12 (57.1%)	

Table IV. Evaluation of diagnostic performance of non-ARMS for different variables

Variables	AUC	95%CI	Sen (%)	Spe (%)
Necrosis	0.690	0.497-0.884	66.7	71.4
Central hyperechoic fiber bundles	0.845	0.694-0.997	83.3	85.7
All clinical characteristics	0.865	0.738-0.992	83.3	76.2
All ultrasound characteristics	0.845	0.694-0.997	83.3	85.7
All clinical and ultrasound characteristics	0.964	0.910-1.000	100	85.7

AUC, area under the curve; CI, Confidence Interval; Sen, sensitivity; Spe, specificity

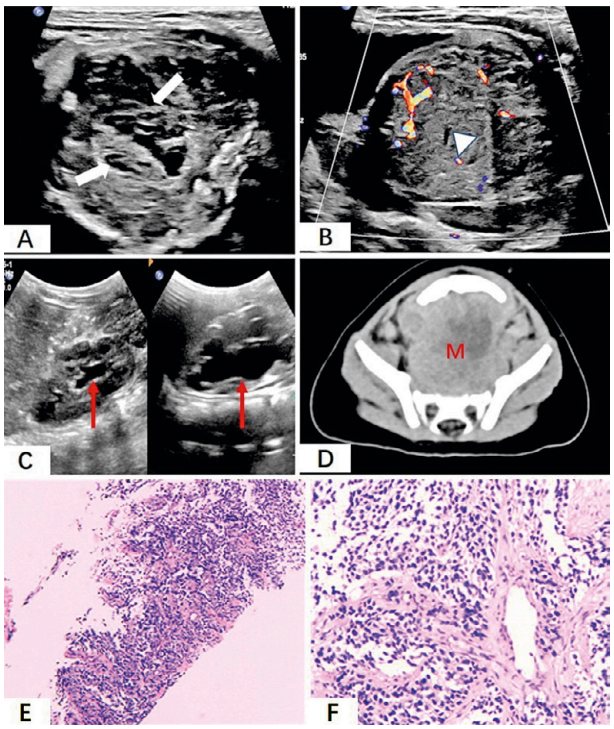

Fig 1. A 6-month-old male infant with a pathological diagnosis of ARMS (TNM stage 3, IRS stage III, risk group intermediate). US revealed a solid echogenic mass in the pelvic cavity, with mixed echogenicity, poorly defined borders, irregular shape, and visible hyperechoic fibrous bundles (A, white arrow) and small areas of necrosis (B, white triangle); CDFI showed Adler grade I, along with bilateral renal pelvic dilation (C, red arrow), suggesting secondary hydronephrosis due to tumor compression; CT revealed a large solid mass in the pelvis with heterogeneous enhancement (D), and final pathology confirmed ARMS, with visible acinar cells (E-F).

originating in the retroperitoneum, pelvis, and limbs are associated with poor prognosis in RMS. Our study confirmed that there were significant statistical differences in location characteristics between the ARMS and non-ARMS groups (p=0.020).

ARMS usually presents with rapidly growing soft tissue masses and corresponding symptoms causing compression of surrounding structures. ARMS are often high-grade lesions, manifesting as invasive, rapidly growing soft tissue tumors. Its biological characteristics

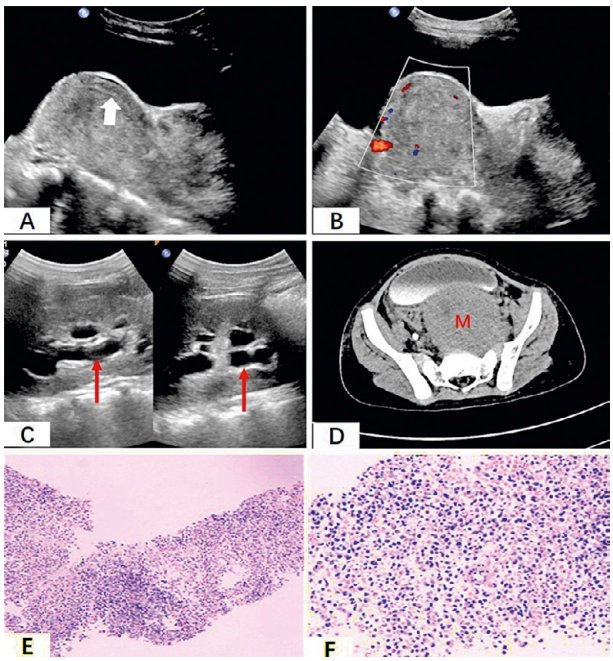

Fig 2. A 9-year-old boy with a pathological diagnosis of ARMS (TNM stage 4, IRS stage IV, risk group high). US revealed a solid hypoechoic mass in the pelvic cavity, compressing the bladder and rectum, with low echogenicity, poorly defined borders, irregular shape, and visible hyperechoic fibrous bundles (A, white arrow); CDFI showed Adler grade I, along with bilateral renal pelvic dilation (C, red arrow) due to tumor compression; CT revealed a large solid mass in the pelvis, multiple nodules in both lungs, and a nodule in the lower chest wall, suggesting tumor metastasis (D). The final pathology confirmed ARMS (E-F).

are far more malignant than ERMS, prone to recurrence and metastasis, and have a lower 5-year survival rate. We found that, compared with the non-ARMS group, the ARMS group showed more TNM stage 4 and IRS stage IV, with higher risk grade and easier distant metastasis. Histologically, ARMS are highly cellular tumors composed of primitive cells with round nuclei, in which fibrous vascular septa divide the tumor cells into nests of varying sizes. These nests contain central cell clusters, giving them an “alveolar” appearance [21]. On the other hand, during gene transcription, the PAX 7-FOXO 1 fusion gene is amplified in most ARMS cases, accom-

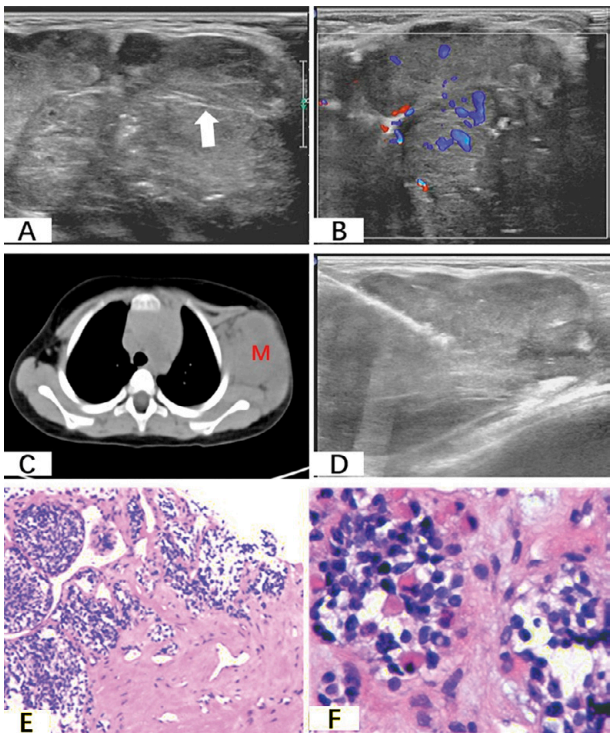

Fig 3. A 1-year-old girl with pathologically confirmed ARMS (TNM stage 3, IRS stage III, risk group intermediate). A hypoechoic subcutaneous muscle layer mass in the left axilla, with unclear borders and a lobulated appearance, containing high-echoic fibrous bundles (A, white arrow); CDFI showed Adler grade III, and CT revealed a soft tissue mass in the left axilla with heterogeneous enhancement (C). The patient underwent ultrasound-guided needle biopsy (D), and the final pathology confirmed ARMS (E-F)

panied by a t (1; 13) translocation, which produces high levels of these chimeric proteins, which activate downstream transcriptional targets, promote cell proliferation and transformation, inhibit cell differentiation and apoptosis, and thus promote tumor development [22,23].

Research indicates that treatment protocols for children RMS should include more detailed imaging guidelines to ensure uniformity in response assessment and better application in practice [24]. The US appearance of RMS in different locations is closely related to its growth site. For example, RMS in the abdominal or pelvic cavity presents as a large mass similar to neuroblastoma or rhabdoid tumor, and the echogenicity of the tumor is closely related to the internal tissue. Tumors arising in the head and neck region may appear adjacent to the parotid gland, orbit, and cervical vessels, the borders of the tumor are not clear, and hypervascular tissues lead to CDFI showing abundant blood flow signals. Paratesticular RMS presents as a large solid mass encapsulating or invading the testis, and Doppler US shows increased vascularity outside the testis and scrotum [25].

We found that there were statistically significant differences between the two groups in necrosis ($p=0.039$) and central hyperechoic fiber bundles ($p<0.001$). Because ARMS is a malignant tumor composed of primitive small round cells, it shows differentiated rhabdomyoblasts with abundant eosinophilic cytoplasm and characteristic neoplastic multinucleated giant cells. Microscopically, it can be observed that the fibrous vascular bundles separate the tumor cells into nests, and the cell adhesiveness in the center of the cell nests is poor, while the peripheral cells are dense [21,26]. We could therefore observe hyperechoic fiber bundles in the center of the tumor rather than pseudocapsule located at the periphery of the tumor in US images. On the other hand, ARMS alveolization is formed because tumor cells accumulate at the edge of the fibrous septa and rhabdomyoblasts adhere to the monolayer. In the central part of this lesion, cells lose this connection and undergo necrosis and degeneration [26]. ARMS is more malignant than other types of RMS, and when the tumor grows too fast and newly generated blood vessels fail to provide enough oxygen and energy, it will cause ischemia and hypoxia in the tumor site and then lead to necrosis, which is generally manifested as local or irregular anechogenicity on US images.

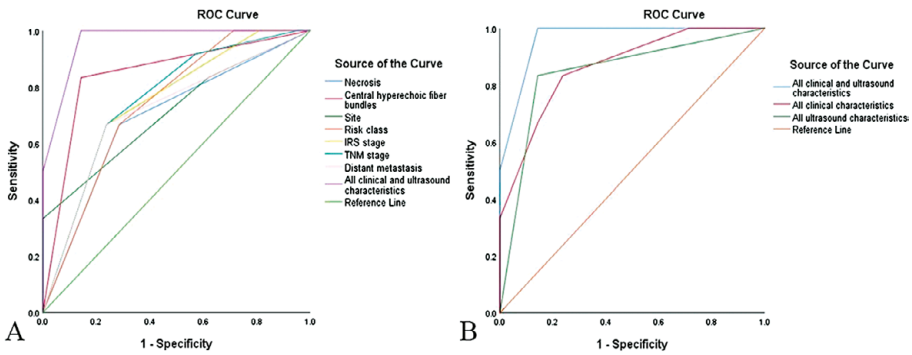

Fig 4. Analyze the diagnostic performance of ARMS based on different variables: A) Compare the ROC curves of different ultrasound features and clinical features; B) Compare the ROC curves of ultrasound features and clinical features combined separately.

This study is the first to systematically compare the US findings of ARMS versus non-ARMS in children from an imaging perspective, providing new evidence for noninvasive preoperative assessment of ARMS. Unlike previous studies that only analyzed single imaging indicators or clinical parameters, this study innovatively combined multiple clinical features with US imaging parameters and verified their diagnostic efficacy by ROC curve, and the results showed that the combined model had significantly higher diagnostic accuracy in ARMS prediction and provided a more operable diagnostic strategy for clinical practice. By clarifying the relationship between ARMS and poor clinical stage, distant metastasis and high-risk grade, combined with US findings, this study provides valuable imaging support for early risk assessment, individualized treatment planning and prognosis of ARMS in children.

Immunohistochemically, ARMS expressed desmin, MyoD1 and myogenin positivity, especially MyoD1 and myogenin showed strong positivity at the edge of the alveolar structure or around blood vessels [27,28]. Clinicians usually identify the nature of the tumor by surgical specimens or needle biopsies. In early diagnosis of RMS, US-guided biopsy can effectively improve the accuracy of sampling. Core needle biopsies are more suitable than fine needle biopsies for assessing morphologic structures and obtaining adequate tissue for cytogenetic and molecular analysis, which may predict aggressive behavior or abnormal gene fusion of the disease [29]. Contrast-enhanced US can further improve the accuracy of preoperative diagnosis of RMS because it can provide blood perfusion and microvascular imaging inside the tumor, while contrast-enhanced US-guided biopsy can also avoid false solid components of two-dimensional images [30]. Although multimodal treatment for RMS has become more established, the overall survival rate is only about 20%. In recent years, immunotherapy and nanomedicine have shown promising results in the treatment of RMS, improving overall survival and causing fewer side effects [31].

This study has some limitations. First, this is a small single-center retrospective study, and the sample size should be expanded for further validation in the future. Second, no prognostic indicator was included in this study because some patients were not treated completely or lost to follow-up during the course of the study; however, we tracked the recurrence and prognosis of hospitalized patients. Therefore, the follow-up time should be prolonged to further verify the correlation between ARMS US images and prognosis in subsequent studies; third, our study is limited to conventional US and Doppler US, and future studies are expected to obtain more information on the internal and molecular levels of the tumor preoperatively with the help of contrast-enhanced US and artificial intelligence to provide more imaging basis for clinical practice.

Conclusions

ARMS has atypical clinical features and poor clinical prognosis in children with ARMS, and combined clinical and US features are helpful for preoperative identification of ARMS and providing imaging evidence for accurate clinical diagnosis and treatment.

Conflicts of interest: none

References

1. Skapek SX, Ferrari A, Gupta AA, et al. Rhabdomyosarcoma. Nat Rev DisPrimers 2019;5:1.
2. Oberoi S, Crane JN, Haduong JH, et al. Children's Oncology Group's 2023 blueprint for research: Soft tissue sarcomas. Pediatr Blood Cancer 2023;70(Suppl 6):e30556.
3. Ognjanovic S, Linabery AM, Charbonneau B, Ross JA. Trends in childhood rhabdomyosarcoma incidence and survival in the United States, 1975-2005. Cancer 2009;115:4218-4226.
4. Jawad N, McHugh K. The clinical and radiologic features of paediatric rhabdomyosarcoma. Pediatr Radiol 2019;49:1516-1523.
5. Choi JH, Ro JY. The 2020 WHO classification of tumors of soft tissue: selected changes and new entities. Adv Anat Pathol 2021;28:44-58.
6. Crane JN, Xue W, Qumseya A, et al. Clinical group and modified TNM stage for rhabdomyosarcoma: A review from the Children's Oncology Group. Pediatr Blood Cancer 2022;69:e29644.
7. Ferrari A, Bernasconi A, Bergamaschi L, et al. Impact of rhabdomyosarcoma treatment modalities by age in a population-based setting. J Adolesc Young Adult Oncol 2021;10:309-315.
8. Spunt SL, Million L, Chi YY, et al. A risk-based treatment strategy for non-rhabdomyosarcoma soft-tissue sarcomas in patients younger than 30 years (ARST0332): a Children's Oncology Group prospective study. Lancet Oncol 2020;21:145-161.
9. Nishida Y, Tsukushi S, Urakawa H, et al. High incidence of regional and in-transit lymph node metastasis in patients with alveolar rhabdomyosarcoma. Int J Clin Oncol 2014;19:536-543.
10. Kubo T, Shimose S, Fujimori J, Furuta T, Ochi M. Prognostic value of PAX3/7–FOXO1 fusion status in alveolar rhabdomyosarcoma: Systematic review and meta-analysis. Crit Rev Oncol Hematol 2015;96:46-53.
11. Raze T, Lapouble E, Lacour B, et al. PAX–FOXO1 fusion status in children and adolescents with alveolar rhabdomyosarcoma: Impact on clinical, pathological, and survival features. Pediatr Blood Cance 2023;70:e30228.

12. Ghayad SE, Rammal G, Ghamloush F, et al. Exosomes derived from embryonal and alveolar rhabdomyosarcoma carry differential miRNA cargo and promote invasion of recipient fibroblasts. Sci Rep 2016;6:37088.
13. Bisogno G, Chisholm J, Hladun R, et al. Maintenance Chemotherapy in Patients With High-Risk Rhabdomyosarcoma: Long-Term Survival Analysis of the European Paediatric Soft Tissue Sarcoma Study Group RMS 2005 Trial. J Clin Oncol 2025;43:1856-1862.
14. Sheng J, Li T, Xu H, et al. Evaluation of clinical and imaging features for differentiating rhabdomyosarcoma from neuroblastoma in children soft tissue. Front Oncol 2024;14:1289532.
15. Franco A, Lewis KN, Lee JR. Pediatric rhabdomyosarcoma at presentation: can cross-sectional imaging findings predict pathologic tumor subtype? Eur JRadiol 2011;80:e446-e450.
16. Lawrence W Jr, Anderson JR, Gehan EA, Maurer H. Pretreatment TNM staging of childhood rhabdomyosarcoma: a report of the Intergroup Rhabdomyosarcoma Study Group. Cancer 1997;80:1165-1170.
17. Raney RB, Maurer HM, Anderson JR, et al. The Intergroup Rhabdomyosarcoma Study Group (IRSG): major lessons from the IRS-I through IRS-IV studies as background for the current IRS-V treatment protocols. Sarcoma 2001;5:9-15.
18. Wang C. Childhood rhabdomyosarcoma: recent advances and prospective views. J Dent Res 2012;91:341-350.
19. Wu J, Shou X, Cai J, et al. Prognostic factors of children pelvic and genitourinary rhabdomyosarcoma: an analysis based on SEER database. Front Oncol 2022;12:992738.
20. Schloemer NJ, Xue W, Qumseya A, et al. Prognosis of children and young adults with newly diagnosed rhabdomyosarcoma metastatic to bone marrow treated on Children's Oncology Group studies. Pediatr Blood Cancer 2023;70:e30701.
21. Agaram NP. Evolving classification of rhabdomyosarcoma. Histopathology 2022;80:98-108.
22. Davicioni E, Graf Finckenstein F, Shahbazian V, Buckley JD, Triche TJ, Anderson MJ. Identification of a PAX-FKHR gene expression signature that defines molecular classes and determines the prognosis of alveolar rhabdomyosarcomas. Cancer Res 2006;66:6936-6946.
23. Barr FG. Gene fusions involving PAX and FOX family members in alveolar rhabdomyosarcoma. Oncogene 2001;20:5736-5746.
24. Schoot RA, Shulkin BL, van Rijn RR, von Kalle T. Pediatric Rhabdomyosarcoma Protocols Should Include More Detailed Imaging Guidelines to Ensure Homogeneous Response Assessment. J Clin Oncol 2023;41:2337-2341.
25. Annam A, Munden MM, Mehollin-Ray AR, Schady D, Browne LP. Extratesticular masses in children: taking ultrasound beyond paratesticular rhabdomyosarcoma. Children radiol2015;45:1382-1391.
26. Dziuba I, Kurzawa P, Dopierała M, Larque AB, Januszkiewicz-Lewandowska D. Rhabdomyosarcoma in children–current pathologic and molecular classification. Pol J Pathol 2018;69:20-32.
27. Kohashi K, Kinoshita I, Oda Y. Soft tissue special issue: skeletal muscle tumors: a clinicopathological review. Head Neck Pathol 2020;14:12-20.
28. Dehner CA, Rudzinski ER, Davis JL. Rhabdomyosarcoma: Updates on classification and the necessity of molecular testing beyond immunohistochemistry. Hum Pathol 2024;147:72-81.
29. Chowdhury T, Barnacle A, Haque S, et al. Ultrasound-guided core needle biopsy for the diagnosis of rhabdomyosarcoma in childhood. Pediatr Blood Cancer 2009;53:356-360.
30. Guo LH, Xu HX, Fu HJ, Sun LP, Liu BJ. Contrast-enhanced ultrasound aids in the detection of prostate rhabdomyosarcoma: A case report and literature review. Oncol Lett 2015;10:1541-1544.
31. Morel VJ, Rössler J, Bernasconi M. Targeted immunotherapy and nanomedicine for rhabdomyosarcoma: The way of the future. Med Res Rev 2024;44:2730-2773.